CHEMICAL CHARACTERIZATION AND REACTIVE OXIDANT POTENTIAL OF INDONESIAN BIOMASS BURNING EMISSIONS

Michael Matthew Williams

A thesis submitted to the faculty at the University of North Carolina at Chapel Hill in partial fulfillment of the requirements for the degree of Master of Science in the Department of Environmental Sciences and Engineering in the Gillings School of Global Public Health.

Chapel Hill
2017

Approved by:

Jason D. Surratt

Barbara J. Turpin

Avram Gold

ABSTRACT

Michael Matthew Williams: Chemical Characterization and Reactive Oxidant Potential of Indonesian Biomass Burning Emissions
(Under the direction of Jason D. Surratt)

Atmospheric fine particulate matter ($PM_{2.5}$) has adverse impacts on air quality, climate, and human health. Primary emissions from biomass burning (BB) in Indonesia can substantially contribute to $PM_{2.5}$ concentrations; however, its chemical composition remains unresolved. In this study, we examined the chemical composition of $PM_{2.5}$ primarily emitted from laboratory burns of Indonesian biomass fuels and ambient $PM_{2.5}$ collected from Singapore when it was influenced by air masses originating from Indonesian peatland fires. We also applied the dithiothreitol (DTT) assay to assess if these samples have oxidative stress potential. We found that laboratory samples generated greater DTT activity compared to previous studies examining diesel particles. Ambient samples generated smaller DTT activity, suggesting that fresh BB-derived $PM_{2.5}$ likely has greater oxidative stress potential than aged BB-derived $PM_{2.5}$. Levoglucosan, an abundant chemical tracer of primary BB emissions, was not associated with DTT activity, suggesting that other primary BB constituents are more DTT active.

ACKNOWLEDGMENTS

First and foremost, I want to thank my wife, Shelley Williams, for her incredible support and dedication to our family while I have been working on this research.

This work would not be possible without the guidance and mentorship of Dr. Jason Surratt. While serving as my advisor, his constant support has been greatly appreciated and I thank him for giving me the opportunity to conduct this work.

I also thank Dr. Sri Hapsari Budisulistiorini and Dr. Mikinori Kuwata for collecting and sending the samples used in this analysis. I also thank Dr. Matthieu Riva for his expertise and assistance with analysis using UPLC/DAD-ESI-HR-TOFMS. I also wish to thank Dr. Ying-Hsuan Lin for guidance and assistance utilizing the DTT Assay methods and calculations.

TABLE OF CONTENTS

LIST OF TABLES vii

LIST OF FIGURES viii

CHAPTER 1: INTRODUCTION 1

CHAPTER 2: MATERIALS AND METHODS 5

Section 2.1. Laboratory Burn Experiments 5

Section 2.2. Ambient Field Sampling 6

Section 2.3. Filter Extraction Procedures 8

Section 2.4. Chemical Characterization of BB Aerosol by Gas Chromatography Interfaced to Electron Ionization-Mass Spectrometry 9

Section 2.5. Complementary Chemical Data 10

Section 2.6. Dithiothreitol (DTT) Analysis 12

CHAPTER 3: CALCULATION APPROACHES 14

Section 3.1. Levoglucosan Quantification Methods 14

Section 3.2. DTT Assay Calculations 15

Section 3.3. Quality Control Methods 17

CHAPTER 4: RESULTS AND DISCUSSION 19

Section 4.1. Chemical Characterization and Tracer Results from Laboratory Burns and Field Samples 19

Section 4.2. DTT Assay Results 26

Section 4.3. Comparison of Chemical Tracers with DTT Activity 28

CHAPTER 5: CONCLUSIONS 29

APPENDIX A: FIELD AND LABORATORY BLANK ANALYSIS 30

APPENDIX B: ORIGINPRO ANALYSIS 31

APPENDIX C: LOCATION OF GC/EI-MS AND DTT ASSAY RAW DATA 32

APPENDIX D: BROWN CARBON SUPPLEMENTAL DATA 34

REFERENCES 37

LIST OF TABLES

Table

1. Types of Fuel Used in Laboratory Burns 8

2. Standard compounds used for calibration and quantification by GC/EI-MS 10

LIST OF FIGURES

Figure

1. Schematic for biomass burning laboratory experiments 7

2. GC/EI-MS calibration curve 14

3. Calibration curve of the 1,4-NQ standard analyzed by the DTT assay 17

4. GC/EI-MS TIC measured from $PM_{2.5}$ collected from laboratory burning of Acacia Mangium 20

5. Aerosol mass concentrations of levoglucosan measured from the laboratory burns 21

6. GC/EI-MS TIC of a $PM_{2.5}$ sample collected during the daytime from Singapore on October 18th, 2015 22

7. Levoglucosan concentrations from October 16-27, 2015..... 23

8. Levoglucosan concentrations measured during 23 h-integrated sampling times 24

9. Ambient organic aerosol mass compared to levoglucosan concentrations 25

10. DTT activity for primary $PM_{2.5}$ samples collected from the laboratory burns 27

11. NIOG values for primary $PM_{2.5}$ samples collected from the laboratory burns 27

12. NIOG values for ambient $PM_{2.5}$ samples collected from haze events 28

CHAPTER 1: INTRODUCTION

Airborne fine particulate matter ($PM_{2.5}$, aerosols with aerodynamic diameters ≤ 2.5 μm) is of growing concern to governments worldwide due to its adverse impacts on local air quality, climate, and human health (Hallquist et al., 2009; Pope and Dockery, 2006). $PM_{2.5}$ can be directly emitted (known as primary aerosol) from anthropogenic activities (e.g., combustion) or natural processes (e.g., volcanic eruptions or wave breaking over oceans). $PM_{2.5}$ can also be indirectly formed through atmospheric chemical oxidation processes; this is known as secondary aerosol. $PM_{2.5}$ is of concern due to the small particle size and its abilities to travel deep into the respiratory system of humans (Xing et al., 2016). The World Health Organization has published warnings and recommendations for concentrations of $PM_{2.5}$ (WHO 2005) and epidemiological studies continue to stress the relevance of exposure to PM and the resulting adverse health effects associated with this exposure (Bell, 2012; Wilhelm et al., 2012). Although understanding the sources and fates of all $PM_{2.5}$ types in the atmosphere is important, anthropogenic sources, such as those through biomass burning activities, are of most concern as the global population continues to grow dramatically, increasing demands on land use for agriculture and urban development. This concern is extremely important to us because of our ability to control these changes by way of regulation and changes in activity levels.

Biomass burning (BB) is the combustion of living or dead organic materials and vegetation. This process can be caused naturally or through anthropogenic means. Large quantities of vegetation are intentionally burned worldwide, and many parts of the developing

world continue to clear land through burning techniques, resulting in 20 to 60 million hectares of land being burned (Crutzen and Andreae, 1990). As climate change continues, warmer and drier conditions are forecasted for many locations (Karl et al., 2009). Primary emissions from BB contributes a large amount of $PM_{2.5}$ into the atmosphere (Crutzen and Andreae, 1990; Bond et al., 2004, 2013). The impacts of BB on local and global climate scales are vast. Trace gases and aerosol emitted by BB increases the global tropospheric ozone burden and decreases global mean OH (Mao et al. 2013). Emissions from fires can also increase warming throughout the globe, and some models have shown that these effects are even greater over the Arctic, decreasing sea ice depth to even further change global weather and climate (Jacobson 2014). Particles emitted by BB also affect the scattering and absorption of solar radiation in the atmosphere (Hobbs et al. 1997).

The numerous chemical compounds emitted during BB events are not well resolved or characterized (Akagi et al., 2011), leading to uncertainties in how primarily emitted particulate and gaseous compounds adversely affect human health and participate in the formation of secondary organic aerosol (SOA). Since BB is the second largest source of non-methane organic compounds emitted into the atmosphere (Bond et al., 2004; Andreae and Merlet, 2001; Forster et al., 2007; Guenther et al., 2006) these compounds have the potential to influence atmospheric chemistry, radiative forcing, and health. For example, they could form low-volatility organic compounds that can nucleate, condense onto pre-existing aerosol, or undergo multiphase chemical reactions to yield SOA. To exhibit the complexity of BB emissions, Hatch et al. (2015) used two-dimensional gas chromatography – time of flight mass spectrometry to analyze laboratory samples of selected biomass fuels. This study tentatively identified over 700 compounds in the different fuel types. Some individual fuel types contained as many as 474

compounds. Various fuel types were also analyzed by Stockwell et al. (2015) and they found widely varying amounts of compounds in different fuel types. The complexity of BB emissions raises many questions about the short- and long-term effects on the global climate and human health.

Many studies have examined the link between ambient particulate matter and negative health impacts (Tao et al., 2003, Li et al. 2003a/b, 2008, Bernstein et al., 2004, Lighty et al., 2011). Some of these same studies have observed positive associations between adverse health and oxidative potential, suggesting a causal relationship (Li et al., 2003a/b, 2008). Due to this possible linkage, studies have set forth goals to determine the oxidative potential of particles, especially ambient particles using the DTT assay (Cho et al., 2005, Li et al., 2009, Verma et al., 2014, 2015, Rattanavaraha et al., 2011, Kramer et al., 2016). The DTT assay is a common method used to attempt to quantify the redox activity of $PM_{2.5}$ samples. It also measures the potential of those samples to generate reactive oxygen species (ROS) (Li et al., 2009). The DTT assay has been used to provide a measure of the redox activity of particles by determining superoxide radical formation (Cho et al., 2005). Additionally, it has been suggested that the consumption rate of DTT by PM samples is related to the particles' ability to induce stress protein formation in cells (Li et al., 2003a).

In this study, we will systematically examine the chemical composition of primary $PM_{2.5}$ derived from laboratory burns of various Indonesian fuel types. We will also examine the chemical composition of $PM_{2.5}$ collected from ambient air in Singapore during haze events that occurred due to direct influence of Indonesian peatland fires. Lastly, we will use a chemical-based toxicological assay (the DTT assay) to determine if primary $PM_{2.5}$ derived from laboratory

burns and the ambient $PM_{2.5}$ from Singapore influenced by Indonesian peatland fires have oxidative stress potential.

CHAPTER 2: MATERIALS AND METHODS

2.1. Laboratory Burn Experiments. Biomass burning experiments were conducted at the Earth Observatory of Singapore, at the Nanyang Technological University in Singapore. Thirteen types of biomass were burned in a laboratory combustion chamber experiment. The types of biomass fuel included peats, ferns, leaves, and charcoal from burned peatland in Indonesia. The biomass was burned in a 100 L stainless steel container at room temperature and atmospheric pressure. Additional details regarding the combustion chamber experiments have been recently described by Budisulistiorini et al. (2017) and are also shown in Figure 1. The fuel was not pre-dried and was burned at 350 ºC using a thermocouple and proportional–integral–derivative (PID) controller for 50-60 min in order to replicate Indonesian peatland fires (Usup et al., 2004, Tropics). The fuel was not weighed before combustion was started. Once burning initiated, the fuel would glow for a period of 1-2 minutes and then smolder for the remainder of the experiment. Particle-free mixing air was added to ensure proper mixing of the smoke from both the glowing and smoldering phases of the burn inside the chamber. The air inside the chamber was then collected 1-2 minutes after combustion was complete. Particle-free air was continuously added to the combustion chamber to main atmospheric pressure during particle sampling. The burns conducted were mostly oxygen starved due to the lack of flames at the time sampling began.

Even though a scrubber to remove gaseous components was not applied during filter sampling, all combustion chamber air samples were collected onto Teflon membrane filters (47

mm in diameter, 0.2-μm pore size, Fluoropore^{TM}) in order to minimize the uptake of gases. The sampling flow rate was 0.5 L min^{-1} for 30–35 min. The filters were wrapped in pre-baked aluminum foil and stored under dark conditions at -20 ºC until analysis. These filters were shipped under frozen and dark conditions to UNC for chemical analyses. The stainless-steel container was wiped clean with Milli-Q water and 2-propanol (industrial grade, Katno Chemical Co., Inc.) at least three times with each solvent after completion of each experiment in order to ensure particles were removed from the inner combustion chamber walls. Due to this cleaning method, there were likely some particles that were not removed in between each burning experiment, and this is a possible limitation in this study.

2.2. Ambient Field Sampling. During the course of a haze episode in Singapore that occurred from October 14-30, 2015, and was heavily influenced by air masses that originated from major peatland fires in Indonesia (see Fig. S1 from Budisulistiorini et al., 2017), ambient aerosol samples were collected through a $PM_{2.5}$ cyclone interfaced to a low-volume particle filter sampler. The $PM_{2.5}$ low-volume filter sampler was operated at 4.2 L min^{-1}. The filter sampling was conducted at two different times using local $PM_{2.5}$ concentrations measured by the National Environment Agency (NEA) in Singapore; one during 23 hours of low ambient $PM_{2.5}$ concentrations ($\leq$ 50 μg m^{-3}) and one during ~ 12 h periods (daytime and nighttime sampling was 08:00-19:45 and 20:00-07:45, respectively, local time) at times of higher ambient $PM_{2.5}$ concentrations (> 50 μg m^{-3}). The ambient $PM_{2.5}$ samples were collected onto pre-baked 47 mm quartz fiber filters. These filters were pre-baked at 250 ºC for 16 h. Filter blanks, or filters placed into the sampler with no air flow, were also collected during the sampling timeframe. The filters were wrapped in pre-baked aluminum foil and stored under dark conditions at -20 ºC.

These ambient $PM_{2.5}$ filter samples were also shipped under frozen and dark conditions to UNC for further chemical analysis.

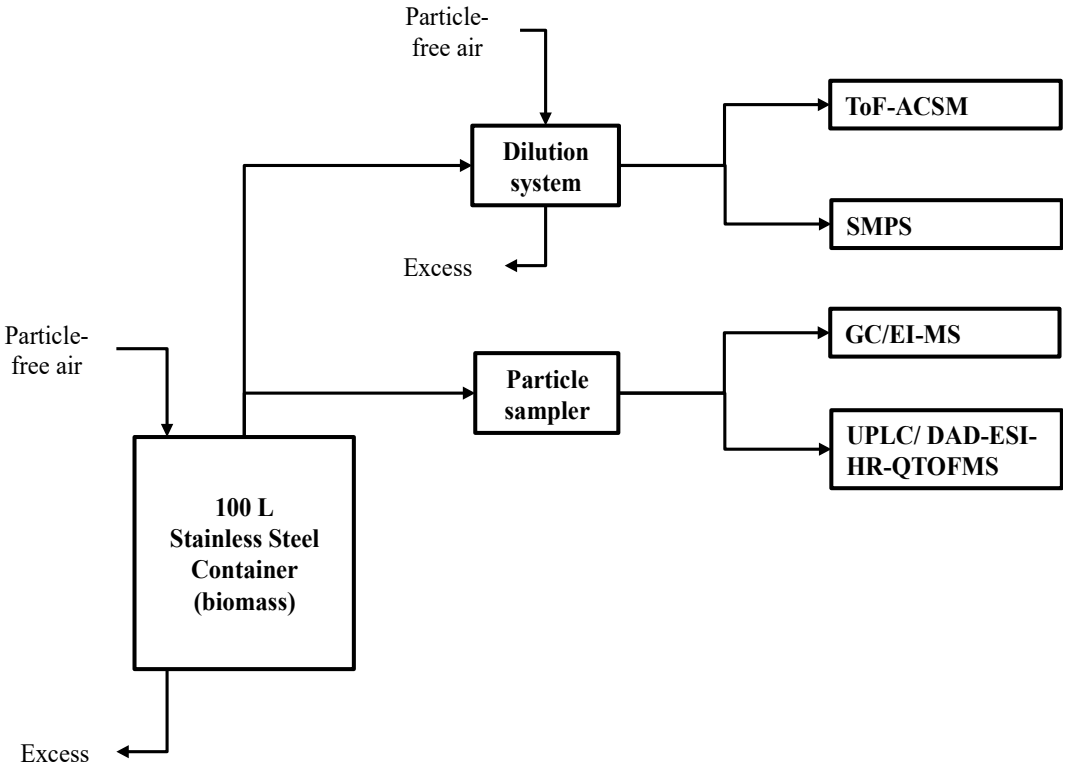

Figure 1. Schematic for BB laboratory experiments.

Table 1. Types of fuel used in laboratory BB experiments.

Fuel	Location	Description
Peat		
KB1 (0 – 10 cm) KB2 (0 – 10 cm; 30 – 40 cm) KB3 (0 – 10 cm) KB4 (0 – 10 cm)	Riau Province, Bengkalis District, Tanjung Leban Village (red star)	Burned area with fern and grass growth
Soil		
Sepahat	Riau Province, Bengkalis District, Sepahat Village (yellow circle)	Secondary forest, not burned
Zamrud	Riau Province, Siak District, Inside the oil company (green circle)	Primary forest
DB (drained burned)	Central Kalimantan Province, Palangkaraya City (orange square)	Drained by canal, burned area
DF (drained forest)	Central Kalimantan Province, Palangkaraya City (orange square)	Drained by canal, unburned forest
Charcoal	Riau Province	
Leaf		
Pteridium (fern)	Riau Province, Bengkalis District, Tanjung Leban Village (red star)	Dried. Collected at location of peat samples
Stenochlaena palustris (fern)	Riau Province, Bengkalis District, Tanjung Leban Village (red star)	Dried. Collected at location of peat samples
Acacia mangium (acacia tree)	Riau Province, Bengkalis District, Tanjung Leban Village (red star)	Dried. Collected at location of peat samples

2.3. Filter Extraction Procedures. Laboratory experiments produced high amounts of organic aerosol mass on filters (5-90 mg m^{-3}) (Budisulistiorini et al., 2017); therefore, laboratory filter samples were cut into fractions (0.5) prior to extracting them for chemical analysis. One half of each filter was placed into a 22 mL scintillation vial and filled with 20 mL of high-purity methanol (LC-MS CHROMASOLV-grade, Sigma Aldrich ≥ 99.9%). These vials were then capped with Teflon caps and then further sealed with polytetrafluorethylene (PTFE) tape to

prevent evaporation. Sealed scintillation vials were sonicated for 45 min. Steps were taken to ensure the samples would not become overheated; specifically, after 25 min of sonication, water inside the sonicator was drained and replaced with fresh, cool water. Sample vials were then sonicated for an additional 20 min. This process was applied to filters obtained from both laboratory burns and Singapore air. After sonication was complete, the methanol containing extracted filter material was transferred to clean 20 mL scintillation vials. The laboratory samples contained insoluble particles, therefore, these extracts were filtered through PTFE syringe filters (Pall Life Science, Acrodisc®, 0.2-μm pore size) in order to remove these free-floating particles. However, syringe filtering was not applied when laboratory filter samples were extracted for analysis by the dithiothreitol (DTT) assay, which is described in more detail in subsequent sections. Due to the presence of quartz fibers, ambient filter extracts were also filtered through PTFE syringe filters to remove any quartz filter fiber residues. After syringe filtering all sample extracts, methanol extracts were blown dry under a gentle N_2 (g) stream at room temperature. For sample extracts analyzed by the DTT assay, they were only dried to 1 mL rather than being completely dried.

2.4. Chemical Characterization of BB Aerosol by Gas Chromatography Interfaced to Electron Ionization-Quadrupole Mass Spectrometry (GC/EI-MS). Dried filter extracts were immediately trimethylsilylated by addition of 100 μL of N,O-bis(trimethylsilyl)trifluoroacetamide (BSTFA) + trimethylchlorosilane (TMCS) (99:1, v/v, Supelco) and 50 μL of pyridine (Sigma-Aldrich, 98%, anhydrous), and heated at 70 C for 1 h. Within 24 h following trimethylsilylation, samples were analyzed by GC/EI-MS at 70 eV (Hewlett 5890 Packard Series II Gas Chromatograph interfaced to a HP 5971A Series Mass Selective Detector, Econo-CapTM-ECTM-5 column, 30 m × 0.25 mm × 0.25 μm). The detailed

operating conditions and temperature program are described elsewhere (Surratt et al., 2010; Lin et al., 2012). Resultant GC/EI-MS total ion chromatograms (TICs) were analyzed in detail for known BB-derived organic molecular tracers. GC/EI-MS TICs of known pure standards, such as levoglucosan which is a well-known BB molecular tracer (Simoneit et al. 1999), were compared to the sample TICs. Table 2 shows all pure compounds used to calibrate and quantify known BB organic tracers characterized in $PM_{2.5}$ samples collected from the laboratory burns and from Singapore.

Table 2. Standard compounds used for calibration and quantification by GC/EI-MS.

Compound	Formula	Remarks
Anhydro sugars		
Levoglucosan	$C_6H_{10}O_5$	commercial
Mannosan	$C_6H_{10}O_5$	commercial
Authentic SOA		
2-methyltetrols	$C_5H_{12}O_4$	synthesized in-house[a]
Organic Acids		
Malic acid	$C_4H_6O_5$	commercial
Pimelic acid	$C_7H_{12}O_4$	commercial
Phthalic acid	$C_8H_6O_4$	commercial
Succinic acid	$C_4H_6O_4$	commercial
Maleic acid	$C_4H_4O_4$	commercial
Adipic acid	$C_6H_{10}O_4$	commercial
Glutaric acid	$C_5H_8O_4$	commercial
Other		
Sucrose	$C_{12}H_{22}O_{11}$	commercial

[a]*Details of organic synthesis can be found in Budisulistiorini et al. (2015).*

2.5. Complementary Chemical Data. The time-of-flight aerosol chemical speciation monitor (ToF-ACSM) was used to quantitatively measure the real-time compositions of non-refractory PM_1 (NR-PM_1) during each of the burning experiments (Fröhlich et al., 2013). In addition to laboratory sampling, the ToF-ACSM also measured the chemical compositions of ambient NR-PM_1 sampled in Singapore between October 10–31, 2015, which directly

overlapped with the ambient $PM_{2.5}$ filter sampling described above. The NR-PM_1 components measured included organic, sulfate, nitrate, ammonium, and chloride. Details of the operating conditions, calibration procedures, and quantification methods were fully described in our recently published work (Budisulistiorini et al., 2017). ToF-ACSM measurements were used to help determine actual organic aerosol (OA) mass loadings on filters. This calculation was done by using the concentration of OA mass in μg m^{-3} multiplied by the sample volume (m^3) for each individual sample.

In addition to ToF-ACSM measurements, $PM_{2.5}$ samples collected from laboratory burns and from Singapore were also analyzed by ultra-performance liquid chromatography interfaced to a diode array detector and a high-resolution quadrupole time-of-flight mass spectrometer equipped with electrospray ionization (UPLC/DAD-ESI-HR-TOFMS) operated in the negative ion mode. Detailed operating procedures for the UPLC/DAD-ESI-HR-TOFMS are described elsewhere (Budisulistiorini et al., 2017; Zhang et al. 2011). The UPLC/DAD-ESI-HR-TOFMS was used to chemically characterize brown carbon (BrC) aerosol constituents, which included nitro-aromatics, oxygenated-conjugated compounds, and sulfur-containing organics, in the $PM_{2.5}$ samples collected from both the laboratory burns and from Singapore, as recently described by Budisulistiorini et al. (2017). This data is found in Appendix D. For UPLC/DAD-ESI-HR-TOFMS quantification, the following authentic standards were used: 2-nitrophenol (Sigma-Aldrich, 98%), 4-nitro-o-cresol (TCI America, > 98%0, 4-nitro-1-naphthol (TCI America, >98%), sinapic acid (Sigma-Aldrich, >98%), sodium octyl sulfate (Sigma-Aldrich, > 95%), and 2-methyltetrol sulfates synthesized in-house using previously published procedures (Budisulistiorini et al., 2015). These BrC aerosol constituent data were used in the current study

in order to determine if DTT activity (or oxidative stress potential) was associated with these important aerosol components that have climatic effects (Laskin et al., 2015).

2.6. Dithiothreitol (DTT) Analysis. The DTT assay was used to determine the potential redox activity of an aerosol sample (Li et al., 2009; Rattanavarha et al., 2011; Verma et al., 2012; Verma et al., 2015; Kramer et al., 2016). The DTT assay was monitored using a U-3300 Hitachi spectrophotometer. The DTT standard (powder form, Sigma-Aldrich) was added to a buffer, as described below, to prepare a fresh 5 mM DDT stock solution daily. After all samples were dried down to 1 mL of methanol filter extract, they were sealed and placed into a -20 ºC freezer to prevent loss due to evaporation. It is noted here that filters were extracted in methanol for the DTT assay since prior work has reported methanol is more effective in extracting redox-active organic components from PM samples than in water (Rattanavaraha et et al., 2011; Verma et al., 2012; McWhinney et al., 2013; Yang et al., 2014). The assay was conducted by first calibrating the system with DTT and 0.01 mg ml^{-1} 1,4-naphthoquinone (1,4-NQ, Sigma-Aldrich). A buffer solution containing 99 mL of 0.05 mol L^{-1} potassium dihydrogen phosphate (KH_2PO_4, pH 7.4, Fisher Scientific) and 1 mL of 1 mM ethylenediaminetetraacetic acid (EDTA, Sigma-Aldrich) is created. To calibrate the system and ensure accuracy, varying solutions of DTT and 1,4-NQ (from 0 µL to 50 µL) were used. First, the final volumes of all standards and samples were 1350 µL to prevent the need to adjust for different volumes. The DTT standards were created using the buffer solution and 0 µL to 50 µL of DTT in six steps of 10 µL. The 1,4-NQ standards were created using the buffer solution and 0 µL to 50 µL of 1,4-NQ in six steps of 10 µL. The 1,4-NQ standards also each contain 50 µL of DTT. These standards were placed into an oven at 37 ºC for 30 min. When the reaction time was reached, 100 µL of 5,5'-dithiobis-(2-nitrobenzoic acid) (DTNB, Sigma-Aldrich) was placed in each standard vial to react with the remaining thiol. 1,4-

NQ was used as an external standard to determine the reactivity of DTT. For all standards, buffer solutions were varied to ensure that final volume of 1350 μL was made, including for DTNB, 1,4-NQ, and DTT. Filter sample vials were created by using 1000 μL of buffer solution, 200 μL of the sample, and 50 μL of DTT. These were also placed in a 37 ºC dry bath for 30 min. After the reaction time was reached, 100 μL of DTNB was placed in each vial. All standards and samples were analyzed within 1 h. Two solvent blanks, one of the buffer solutions only, and another blank of the buffer solutions containing methanol only, were also analyzed. In sample analysis, it was determined that BrC constituents in the samples were contributing an interference in the measurements of DTT activity. This was corrected for by measuring the absorbance at 412 nm of the sample only in the solutions of buffer and DTNB (without any DTT added). This absorbance was then compared to the baseline of the buffer alone, and then subtracted from the absorbance of the sample measured with DTT in solution to give a corrected value without the BrC interference.

CHAPTER 3: CALCULATION APPROACHES

3.1. Levoglucosan quantification methods. Levoglucosan was quantified in all samples using multiple data sets. Calibration factors for levoglucosan were determined by creating a standard calibration curve using commercially-available levoglucosan (99% pure, Sigma-Aldrich). Varying solutions of levoglucosan were created and analyzed via GC/EI-MS. Extracted ion chromatograms (EICs) at *m/z* 204, which is a major fragment ion for levoglucosan, were integrated for each calibrant solution, laboratory burn sample, and ambient samples collected from Singapore.

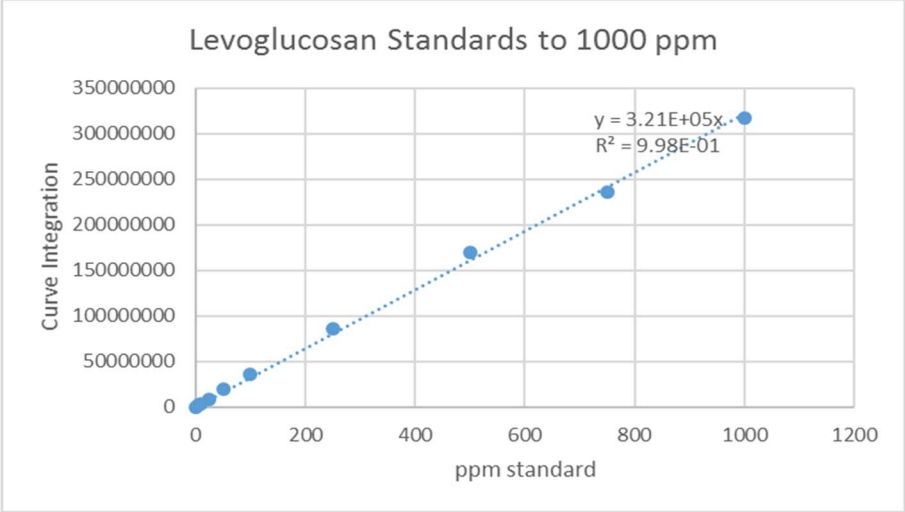

Figure 2. GC/EI-MS calibration curve demonstrating a linear-dynamic range up to 1000 ppmv for levoglucosan quantification.

The peak area was integrated for each EIC at *m/z* 204 collected for each sample and used in the following series of calculations to determine the aerosol mass concentration of the levoglucosan.

$$ppm = \frac{gram\ species}{10^6 gram\ total\ mass}$$

$$\rho\ (solv) = \frac{1\ g}{mL}\ with\ 0.15\ mL\ of\ solvent$$

$$= \left(\frac{\cancel{gram}\ species}{\cancel{10^6 mL\ solvent}}\right)(0.15\ \cancel{mL\ solvent})\left(\frac{\cancel{10^6}\mu g}{\cancel{g}}\right)$$

$$= \frac{0.15\ \mu g\ species}{(EE_{frac})(V_{samp} in\ m^3)(Filt.\ Frac.)} = \frac{\mu g}{m^3}$$

Solvent density was assumed to be 1 g mL^{-1}. The sampling volume was calculated using the sampling time and the flowrate of the air being sampled onto the filters. Extraction efficiency (EE_{frac}) was calculated by using lab blank filters spiked with levoglucosan and empty vials spiked with the same concentration of levoglucosan, then calculating a fraction of levoglucosan obtained from the filters when applying the full extraction process. For the purposes of this experiment, the EE_{frac} was determined to be 98% for levoglucosan. The filter fraction (Filt. Frac.) is the fraction of the original filter size used during the extraction process. In these experiment, one half of the laboratory filter samples were extracted, whereas one quarter of the field filter samples were extracted. This decision was made due to the availability of filter material and estimated mass from ToF-ACSM measurements, allowing for repeat procedures if needed.

3.2. **DTT Assay calculations.** Oxidative stress potentials were calculated and expressed as DTT activity (nmol of DTT consumed/min/μg sample) and as the normalized index of oxidant generation (NIOG) for comparison with previously published studies. DTT consumed is calculated using the slope and intercept of the DTT calibration curve and the absorbance of the

sample. DTT activity is then calculated using the DTT consumed over 30 min of reaction time per microgram of sample analyzed. Furthermore, Li et al. (2009) calculates and describes the use of NIOG as the percentage of absorption decrease min^{-1} μg^{-1} of sample, normalized by the index of oxidation generation (IOG) for the 1,4-NQ standard. This was calculated using the following equation:

$$NIOG_{sample} = \frac{IOG_{sample}}{IOG_{1,4-NQ}}, \quad where\ IOG = \frac{(Abs_0 - Abs')}{Abs_0} * \frac{100}{T*M}$$

Abs_0 is the absorbance detected in the UV Spectrophotometer at 412 nm for a standard only containing 50 µL of DTT; this is both the 50 µL DTT standard and the 0 µL 1,4-NQ standard, and as a result, the absorbance should be similar. Abs' is the absorbance detected at 412 nm of the sample being measured. T is the reaction time with DTT. During this experiment, the samples would react with DTT for 30 min. M is the mass of aerosol used for this assay and was estimated using the OA mass concentration measured by the ToF-ACSM multiplied by the filter sampling volume. This mass was then divided by the fraction size of the filter extracted. M varied for each filter sample during the DTT assay experiments, especially since some filters had much greater mass than others. The IOG of 1,4-NQ was determined from the standard calibration curve of 1,4- NQ, using a value that matched the slope of the curve.

One-way analysis of variance (ANOVA) followed by post hoc Fisher's Least Significant Difference (LSD) tests were applied to test the significance of differences between laboratory burn extracts. $P < 0.05$ was considered statistically significant. Significant differences were found in 5 out of the 10 laboratory samples, KB3, KB4, Narrowleaf, Char, and Zamrud. The analysis for this was conducted using OriginPro, and the results are attached in Appendix B.

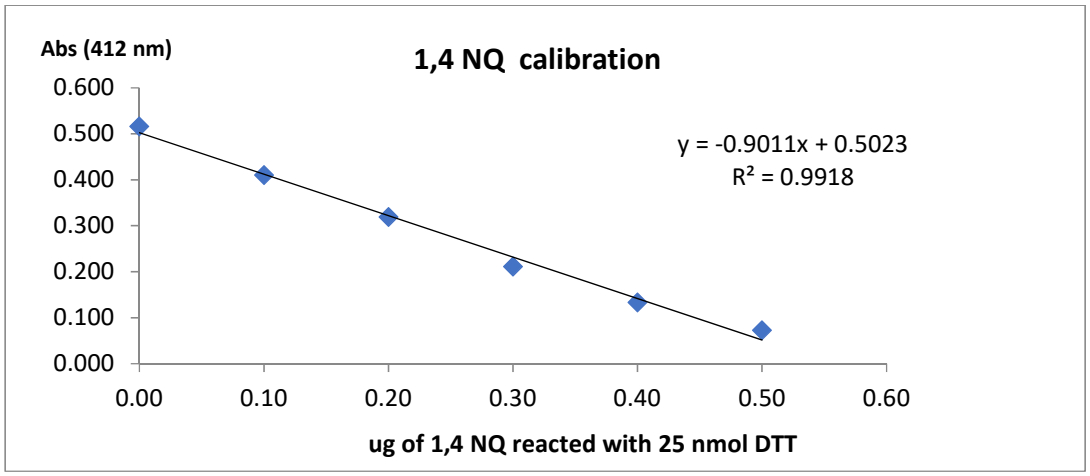

Figure 3. Calibration curve of the 1,4-NQ standard analyzed by the DTT assay.

3.3. Quality Control Methods. Blank filters were also collected for laboratory burn experiments and during the ambient sampling period. Air was not pulled through these blank filters; however, all blank filters were prepared, handled and analyzed in the same manner as the experimental samples. Blank filter analysis results using GC/EI-MS are shown in Appendix A, Figures A1-A2. All blank filters analyzed showed no abundance of levoglucosan with mass to charge (*m/z*) of 204 in the EIC. The detection limit of levoglucosan found in this analysis was 0.1 ppmv. Continuous analysis of standards of levoglucosan was conducted throughout the timeframe of analysis for all filter samples to ensure similar calibration factors were used in all calculations. Levoglucosan calibration coefficient response factors were found to be $3.21 \times 10^{-5} \pm 1.14 \times 10^{-5}$. Solvent blanks were utilized to flush the GC column in between samples to prevent remnants of previous samples appearing on each experiment. Error bars in graphs were estimated based on multiple experiments conducted with levoglucosan standards during the analysis. Standards from 0.5 ppm to 1000 ppm were run each time before analysis, and standard deviations were derived from these standards.

Additionally, blank filter analysis was conducted using the DTT assay. The blank filters

showed no excess DTT consumption, showing values consistent with the standards of 50 μL of DTT (0.498 absorbance at 412nm). This is expected as no materials in the filter blanks are expected to be DTT active. Solvent blanks using only methanol were analyzed in the DTT as well, and the absorbance values of these blanks (0.498 absorbance) also matched the absorbance found in the 50 μL DTT standard used in these calculations.

CHAPTER 4: RESULTS AND DISCUSSION

4.1. Chemical Characterization and Tracer Results from Laboratory Burns and Field Samples.

The laboratory burns of Indonesian biomass fuels yielded very complex total ion chromatograms (TICs). Figure 4 shows a TIC for the broadleaf sample (acacia mangium). This TIC has a similar level of complexity as compared to previous two-dimensional (2-D)-GC/ToF-MS results obtained by Hatch et al. (2015). TICs obtained from $PM_{2.5}$ collected from all laboratory burns had similar complexity. The most abundant compound found using this extraction method in all burns was levoglucosan, explaining 2-75 % of the total OA mass measured by the ToF-ACSM. Utilizing more traditional extraction methods may produce different results, as different compounds may be extracted from the filter materials. Filters extracted using dicholoromethane or hexane may provide greater insight into polar compounds released in primary emissions (Simoneit et al., 1999). Previous studies (Schauer et al., 2001) have found levoglucosan fractions as high as 46% in pine wood burned during fireplace combustions. The different fuel types analyzed by this method contribute a greater fraction of levoglucosan. Due to its high abundance in $PM_{2.5}$ obtained from laboratory burning of Indonesian biomass, levoglucosan was quantified and used as a tracer for primarily emitted BB derived $PM_{2.5}$ in the ambient field samples collected from Singapore.

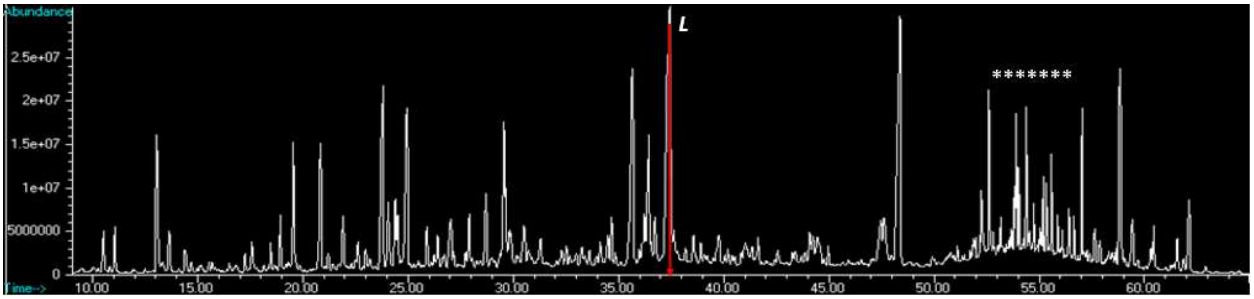

Figure 4. GC/EI-MS TIC measured from $PM_{2.5}$ collected from laboratory burning of Acacia Mangium. Levoglucosan is labeled as L at 37.45 min retention time. The * indicate peaks that are filter artifacts and are not a part of the analysis.

The quantity of levoglucosan measured from each sample varied greatly between different fuel types. The KB1 (peat with fern and grass) and the Narrowleaf (Stenochlaena palustris or fern) had the least amount of levoglucosan (0.51 and 4.37 mg m^{-3}, respectively, or 2 and 14 %, respectively, of total OA mass measured by the ToF-ACSM), while the Broadleaf (Acacia Mangium) had the highest fraction (12.63 mg m^{-3} or 75 % of total OA mass measured by the ToF-ACSM). Figure 5 shows the exact aerosol mass concentrations of levoglucosan measured from the laboratory burns of the various types of Indonesian biomass fuels examined in this study.

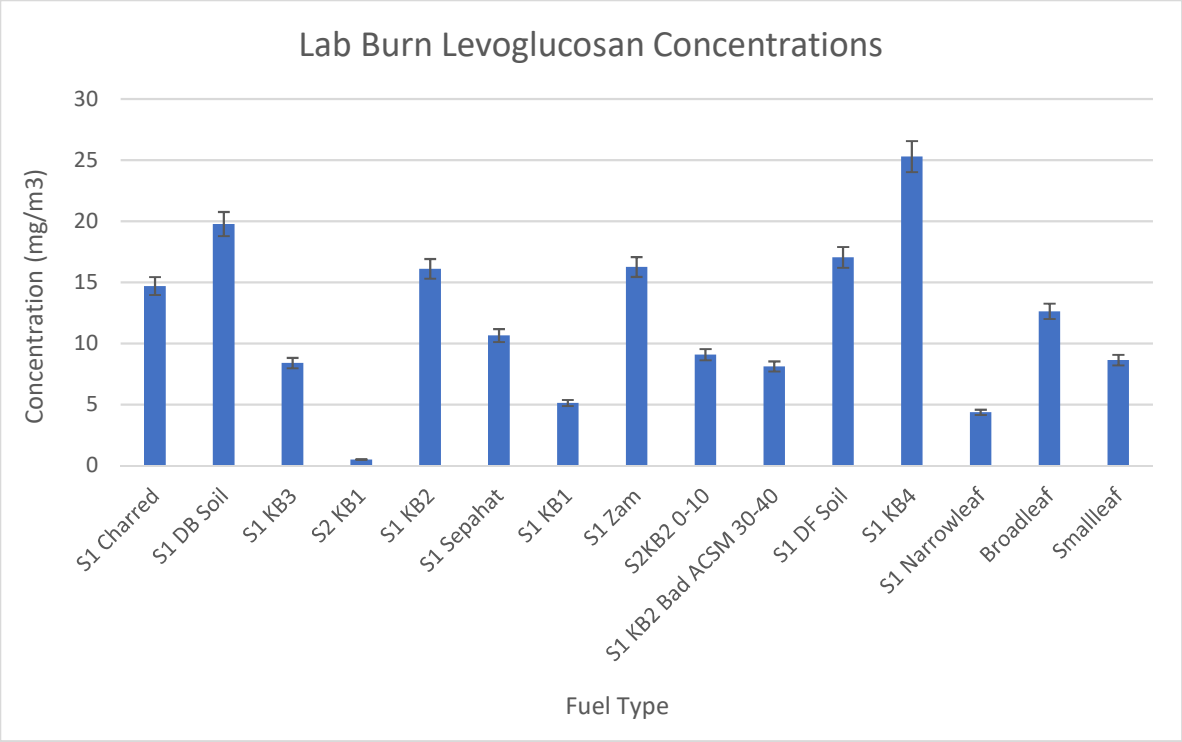

Figure 5. Aerosol mass concentrations of levoglucosan measured from the laboratory burns of the various types of Indonesian biomass fuels examined in this study. Blanks were found to have no levoglucosan present and were not subtracted for this analysis.

Levoglucosan was also quantified in the ambient $PM_{2.5}$ filters samples. Levoglucosan was the most abundant compound during most sampling days in Singapore, supporting that BB had a direct impact on air quality in this region. Figure 6 shows a GC/EI-MS TIC measured from the daytime sample taken on October 18th, 2015. Levoglucosan is the most abundant compound (1.81 μg m^{-3} or 3 % of the total OA mass measured by the ToF-ACSM) found in this sample. The group of chromatographic peaks on this TIC starting around 52 min are derived from filter artifacts. Blank filter TICs can be seen in the appendix section (Appendix A).

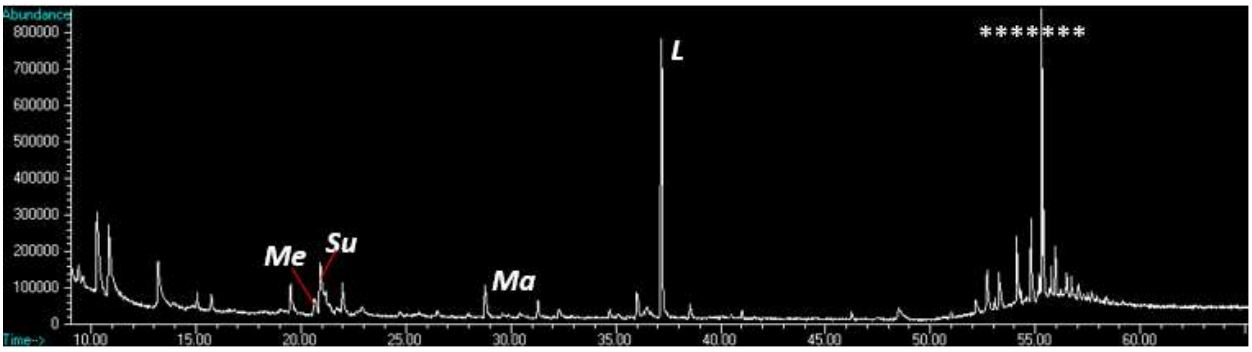

Figure 6. GC/EI-MS TIC of a $PM_{2.5}$ sample collected during the daytime from Singapore on October 18th, 2015. Chromatographic peaks are labelled as follows: levoglucosan (L, R.T. = 37.44 min), maleic Acid (Me, 21.1 min), succinic Acid (Su, 22.01 min), malic Acid (Ma, 27.8 min). (*) indicate species measured on blank filters that are not due to ambient aerosol constituents.

Other major chromatographic peaks in the TICs of ambient field samples are associated with maleic, succinic, and malic acids. These compounds are known to be derived from aromatic oxidations (Kleindienst et al., 2004), and thus, likely are derived from local urban emissions in Singapore or formed from atmospheric chemical aging of aromatics emitted from BB. The summed abundances of these compounds were low or a low fraction of OA mass (~ 0.01 – 1.80 μg m^{-3}, or 0 – 0.5 % of the total OA mass measured by the ToF-ACSM) throughout the sampling period in Singapore. Figure 7 shows the daytime versus nighttime trends of levoglucosan concentration in $PM_{2.5}$ collected from Singapore. The ambient haze was sampled for 11 h during the day and night; 1 h was needed to clean and prepare the sampler for the next sampling period. The three most abundant levoglucosan concentrations were measured on October 18 (1.81 μg m^{-3}), 23 (1.83 μg m^{-3}), and 26 (2.76 μg m^{-3}). Comparing these levels to ambient data taken from other studies showed elevated levoglucosan concentrations in our analysis, likely due to the influence of peatland smoke from Indonesia. For example, Hu et al. (2013) found trace levels (from 0.18 ng m^{-3} to 41 ng m^{-3}) of levoglucosan in ambient air globally. Additionally, Zhang et

al. (2008) studied ambient levoglucosan concentrations in $PM_{2.5}$ in Beijing and found much lower concentrations compared to this study (0.108 μg m^{-3} to 0.806 μg m^{-3}). Another study conducted on a small island in the North Pacific by Mochida et al. (2010) found ambient levoglucosan concentrations that were still quite low compared to this study (0.45 ng m^{-3} to 15 ng m^{-3}).

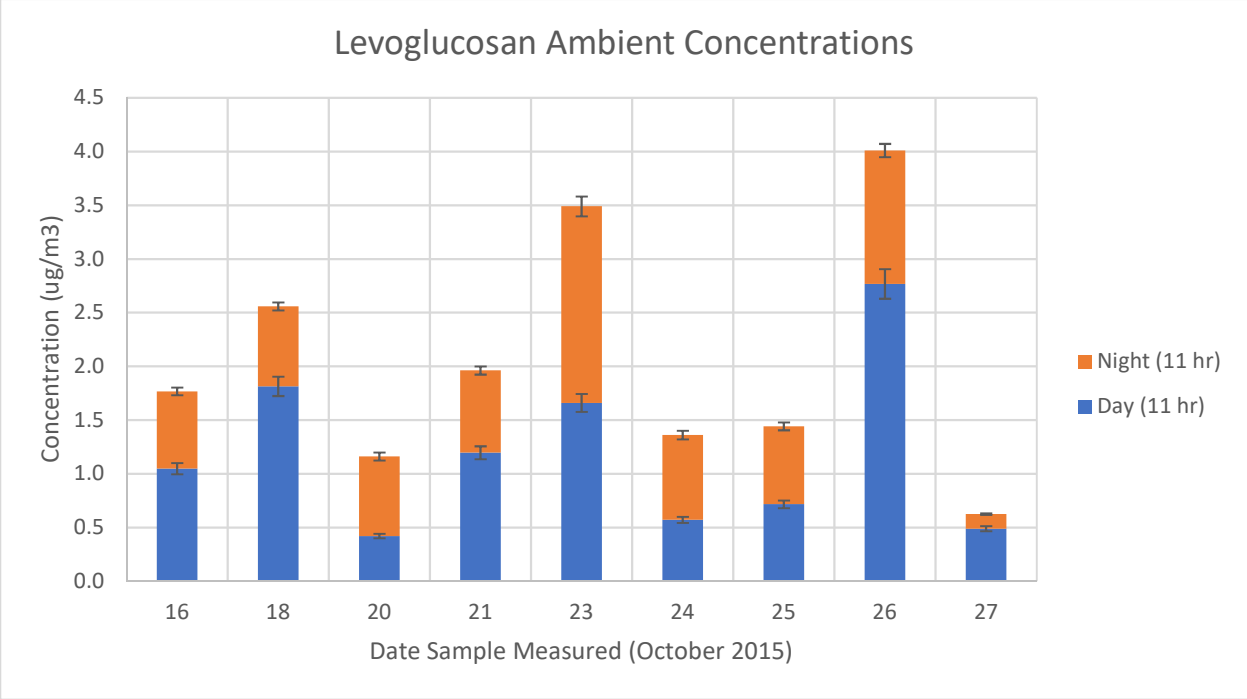

Figure 7. Levoglucosan concentrations measured during the day (11 h-integrated sample) and the night (11 h-integrated sample) from October 16-27, 2015. Blanks were found to have no levoglucosan present and were not subtracted for this analysis.

Additional samples were measured during 23 h-integrated sampling periods in between the day and night rotations. The levoglucosan aerosol mass concentrations from these samples are shown in Figure 8. Levoglucosan concentration peaked on October 19, 2015. In all ambient samples, levoglucosan concentrations were much lower than the primary emissions from the laboratory burn samples. Hennigan et al. (2010) studied the stability of levoglucosan in the

atmosphere, specifically when exposed to hydroxyl radicals. This study observed decay in levoglucosan in particles exposed to OH. The decay ranged from 20% to 90%, and they determined an atmospheric lifetime of 0.7 to 2.2 days when exposed to 1.0 x 10^6 molecules cm^{-3} of OH, which was typical during the summertime when they conducted this analysis. This atmospheric aging process of levoglucosan could partly explain smaller concentrations of levoglucosan typically measured downwind of BB events.

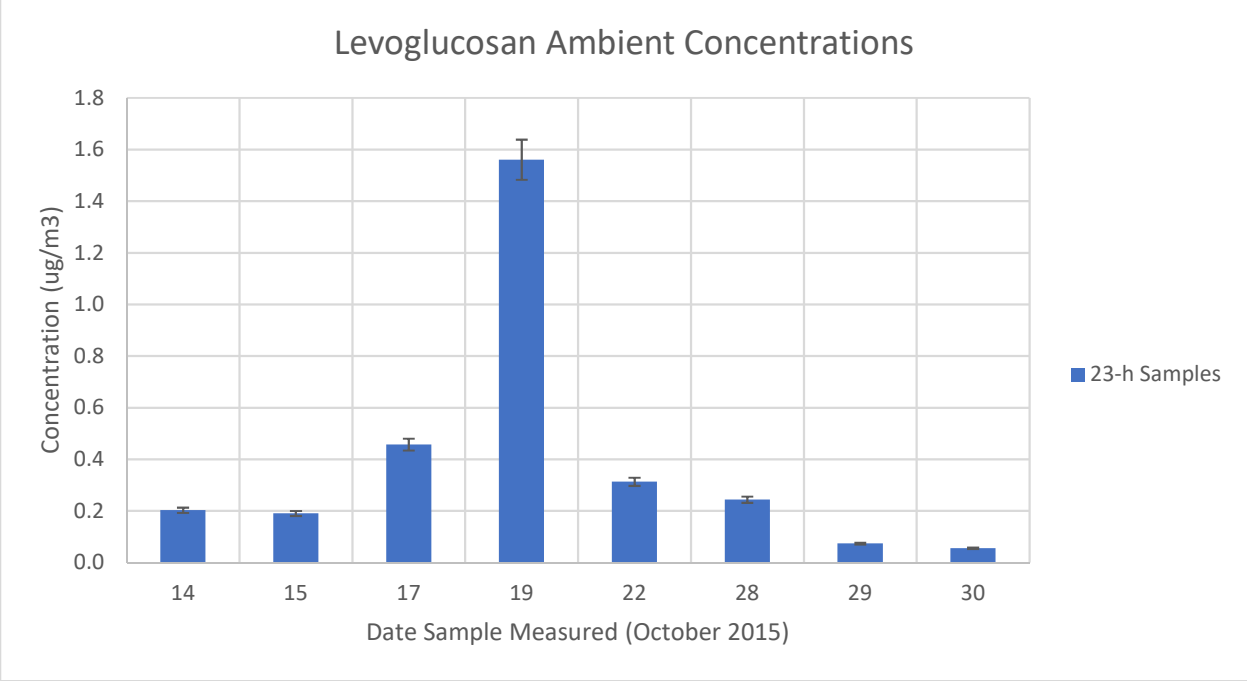

Figure 8. Levoglucosan concentrations measured during 23 h-integrated sampling times. Blanks were found to have no levoglucosan present and were not subtracted for this analysis.

Additionally, levoglucosan concentrations shown in Figure 8 were compared with 23-h integrated OA mass measured by the ToF-ACSM at the same sampling site. The ambient OA mass measured by ToF-ACSM was compared to the levoglucosan measurements from the samples analyzed by GC/EI-MS in Figure 9. Ambient haze pollution events in the area are likely

influenced by BB emissions arriving from peatland fires in nearby Indonesia since levogluosan and OA mass concentrations are well correlated ($r^2 \sim 0.71$).

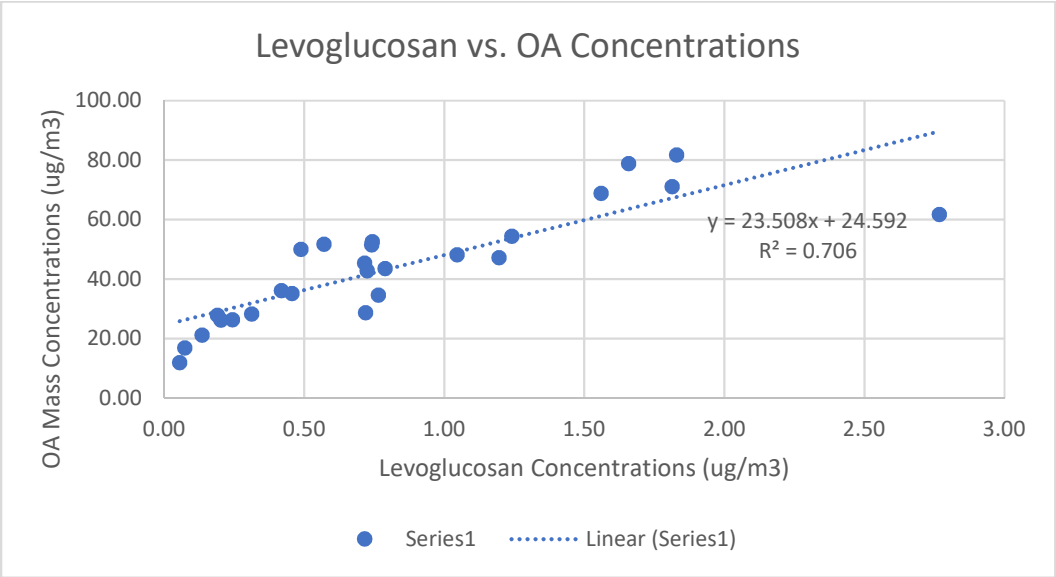

Figure 9. ToF-ACSM measurements of ambient organic aerosol mass during the sampling timeframe compared to levoglucosan concentrations measured by GC/EI-MS.

In addition to the GC/EI-MS results discussed above, we identified 41 individual BrC compounds, such as oxygenated-conjugated compounds, nitro-aromatics, and S-containing compounds, in laboratory-generated $PM_{2.5}$ that can potentially absorb at near-UV and visible wavelengths by using UPLC/DAD-ESI-HR-QTOFMS. The sum of BrC constituents in peat, fern/leaf, and charcoal burning aerosols are 16%, 35%, and 28% of the OA mass, respectively, giving an average OA mass contribution of 24%. Combining the mass of the BrC constituents with the levoglucosan concentrations in the laboratory burns in this study, this accounts for 12 – 100% of the OA mass, with an average of 54%. On average, the BrC constituents account for 0.4% of the ambient OA mass; however, large uncertainties in mass closure remain due to the lack of authentic standards. Details of these measurements have been recently summarized by

Budisulistiorini et al. (2017). Although this recent study highlights the potential of light-absorbing BrC OA constituents from peat, fern/leaf, and charcoal burning, and their importance in the atmosphere, we use this data here to examine their potential association with DTT activity (or oxidative stress potential) measured from $PM_{2.5}$ filter samples collected from laboratory burns and from Singapore.

4.2. **DTT Assay Results.** NIOG values were calculated for all laboratory and ambient field samples. $PM_{2.5}$ samples collected from the laboratory burns showed considerable amounts of DTT activity (3.74×10^{-3} nmol DTT/min/μg sample to 1.94×10^{-2} nmol DTT/min/μg sample) as seen in Figure 10, and, thus, NIOG values (4.48×10^{-3} to 2.36×10^{-2}) as seen in Figure 11. Rattanavaraha et al. (2011) used a similar method to determine NIOG values for fresh and aged diesel exhaust particles. Comparing our NIOG values to this previous study reveals that NIOG values of the primary $PM_{2.5}$ collected from laboratory burns of Indonesian fuels are higher than those measured for fresh and aged diesel exhaust primary particles. NIOG values obtained from $PM_{2.5}$ collected from the laboratory burns are shown in Figure 10 and are compared with those values previously reported by Rattanavaraha et al. (2011) and from isoprene SOA (Kramer et al., 2016). Isoprene-derived SOA had NIOG values (1.79×10^{-3} to 3.13×10^{-3}) smaller than those reported here for the laboratory burns of Indonesian biomass. Fresh and aged diesel particles as described in Rattanavaraha et al. (2011) had NIOG values that were smaller as well (1.0×10^{-3} to 4.0×10^{-3}). This suggests that the chemical compositional differences may explain this trend and is further discussed below. Additionally, Vreeland et al. (2016) analyzed the DTT activity of roadside trash burning in India. The range of values for DTT activity (1.0 to 68.2

pmol/min/μg_{OC}) in their analysis were comparable or slightly higher to the results found in this study (4.47 to 19.43 pmol/min/µg sampled).

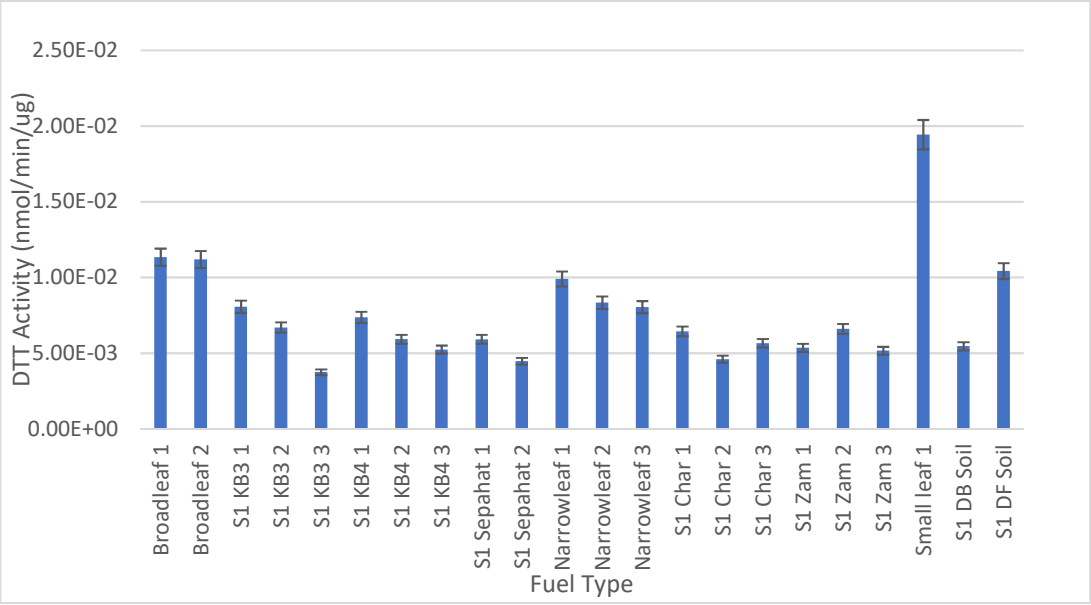

Figure 10. DTT activity (nmol/min/µg sampled) values for primary $PM_{2.5}$ samples collected from the laboratory burns of various Indonesian biomass fuel types.

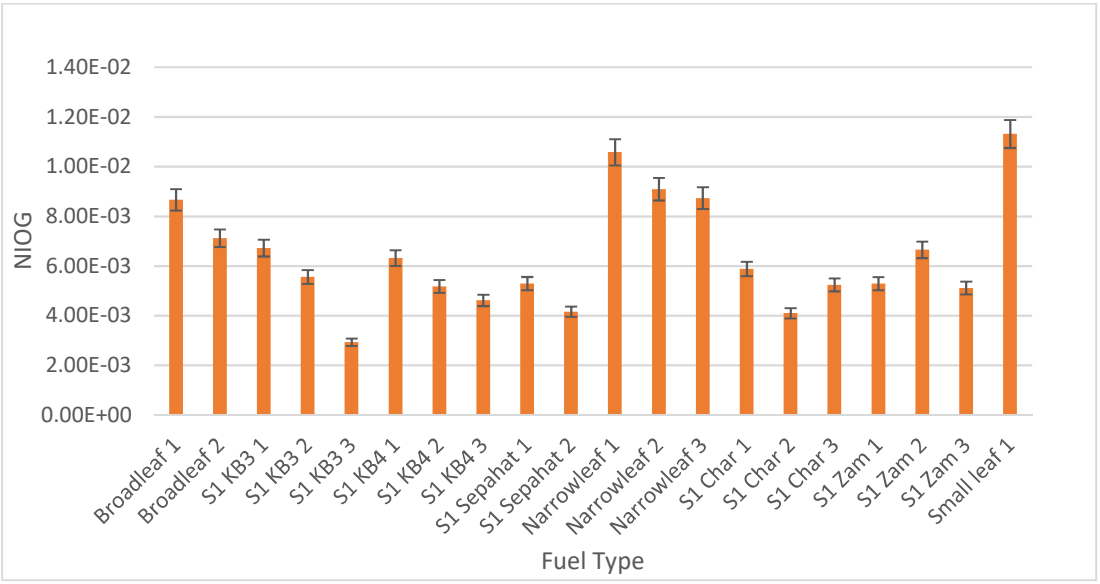

Figure 11. NIOG values for primary $PM_{2.5}$ samples collected from the laboratory burns of various Indonesian biomass fuel types.

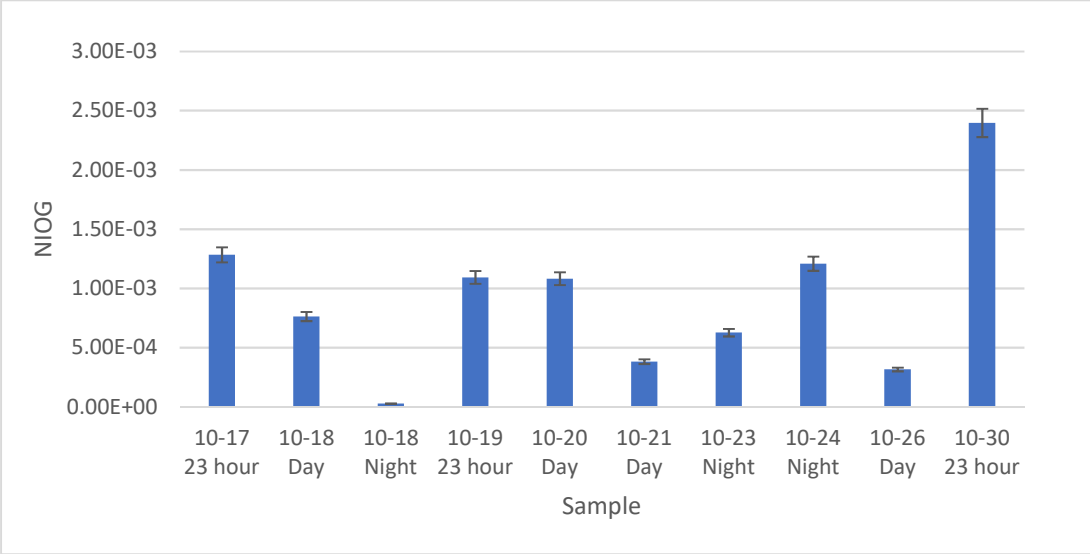

Figure 12. NIOG values for ambient $PM_{2.5}$ samples collected from the haze events affecting Singapore from Indonesian peatland fires.

Figure 12 shows the NIOG values for the ambient samples. These values are lower (from 2.06×10^{-5} to 2.40×10^{-3}) than previous studies conducted on ambient PM data (Verma et al. 2015). Additionally, during DTT analysis of the ambient field samples, no difference was noted between days of high levoglucosan concentration and days with low concentrations. Levoglucosan concentration did not appear to have a relationship to DTT activity or NIOG.

4.3. Comparison of Chemical Tracers with DTT Activity. There was no significant relationship found between the levels of DTT activity in any sample and the levoglucosan concentration found in those samples. This is expected as levoglucosan is not very reactive with DTT and is quite stable (with a lifetime on the order of days) in the atmosphere (Verma et al., 2009). Additionally, DTT activity was compared with BrC constituents from Budisulistiorini et al. (2017) and no significant relationship was found.

CHAPTER 5: CONCLUSIONS

GC/EI-MS is a proven method for analyzing chemical composition of primary BB emissions (Lauraguais et al. 2014, Poster et al. 2006). The single most abundant compound found in the primary $PM_{2.5}$ collected for the laboratory burns was levoglucosan using this filter extraction method, which has been described in previous studies as a fresh BB tracer (Simoneit et al., 1999). Alternative methods of extraction may produce other results when examining the abundance of compounds in these emissions. In ambient $PM_{2.5}$ samples collected during periods in Singapore that were affected by air masses arriving from peatland fires in nearby Indonesia, levoglucosan was also the most abundant compound detected. As a result, measurement of this primary BB tracer in ambient haze in Singapore indicated the influence of BB events.

Additionally, laboratory burn experiments measured using the DTT assay showed much higher levels of NIOG, and oxidative stress potential, than in previous studies with aged diesel exhaust. The DTT activity and NIOG calculations for the ambient samples were much lower than the laboratory samples. Compared to values in Verma et al. (2012, 2015) and Rattanavaraha et al. (2011) the values were overall lower than ambient samples taken in previous studies.

APPENDIX A
FIELD AND LABORATORY BLANK ANALYSIS

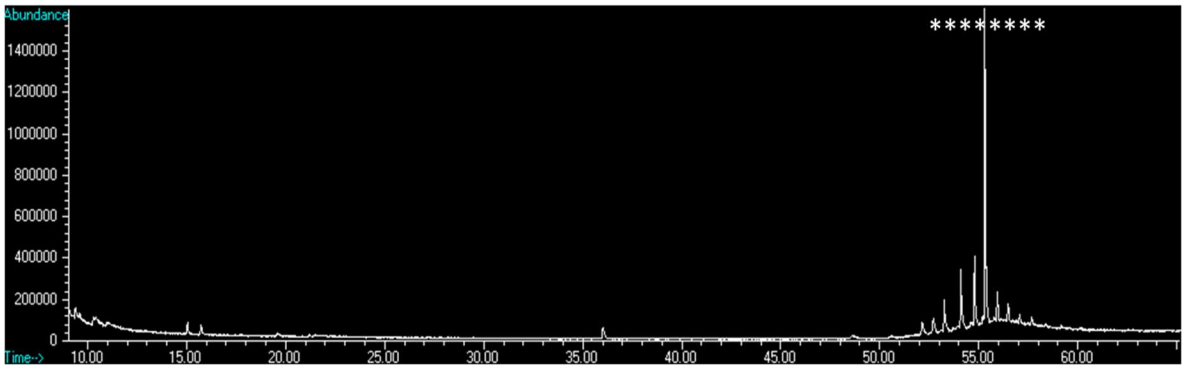

Figure A-1. Total Ion Chromatogram (TIC) of field blanks taken using the ambient air sampling equipment. Asterisks (*) represent filter artifacts.

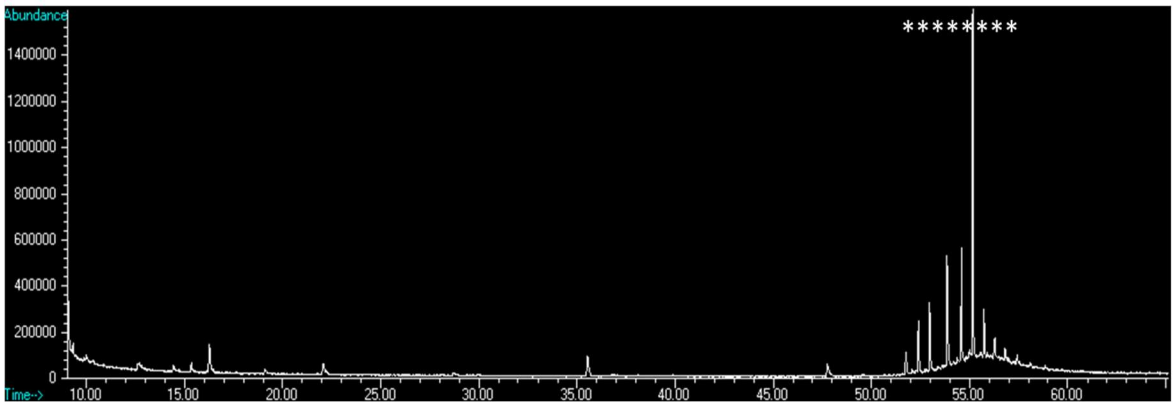

Figure A-2. TIC of laboratory blank filters taken using the laboratory sampling equipment. Asterisks (*) represent filter artifacts.

APPENDIX B
ORIGINPRO ANOVA AND LSD ANALYSIS

ANOVAOneWay (3/28/2017 10:53:13)

Notes

Description	Perform One-Way ANOVA
User Name	Ying-Hsuan Lin
Operation Time	3/28/2017 10:53:13
Report Status	New Analysis Report

Input Data

	Data	Range
S1 KB3	[Book1]Sheet1!B"S1 KB3"	[1*:3*]
S1 KB4	[Book1]Sheet1!C"S1 KB4"	[1*:3*]
Narrowleaf	[Book1]Sheet1!D"Narrowleaf"	[1*:3*]
S1 Char	[Book1]Sheet1!E"S1 Char"	[1*:3*]
S1 Zam	[Book1]Sheet1!F"S1 Zam"	[1*:3*]

Descriptive Statistics

	N Analysis	N Missing	Mean	Standard Deviation	SE of Mean
S1 KB3	3	0	0.00747	0.00272	0.00157
S1 KB4	3	0	0.00749	0.00134	7.71906E-4
Narrowleaf	3	0	0.01065	0.00123	7.12831E-4
S1 Char	3	0	0.0067	0.00114	6.55534E-4
S1 Zam	3	0	0.00691	9.64546E-4	5.56881E-4

One Way ANOVA

Overall ANOVA

	DF	Sum of Squares	Mean Square	F Value	Prob>F
Model	4	3.10477E-5	7.76192E-6	3.00156	0.07223
Error	10	2.58596E-5	2.58596E-6		
Total	14	5.69073E-5			

Null Hypothesis: The means of all levels are equal.
Alternative Hypothesis: The means of one or more levels are different.
At the 0.05 level, the population means are not significantly different.

Fit Statistics

	R-Square	Coeff Var	Root MSE	Data Mean
	0.54558	0.20503	0.00161	0.00784

Means Comparisons

Fisher Test

	MeanDiff	SEM	t Value	Prob	Alpha	Sig	LCL	UCL
S1 KB4 S1 KB3	2.06771E-5	0.00131	0.01575	0.98775	0.05	0	-0.0029	0.00295
Narrowleaf S1 KB3	0.00319	0.00131	2.42586	0.0357	0.05	1	2.59609E-4	0.00611
Narrowleaf S1 KB4	0.00316	0.00131	2.41011	0.03668	0.05	1	2.38932E-4	0.00609
S1 Char S1 KB3	-7.70618E-4	0.00131	-0.58691	0.57027	0.05	0	-0.0037	0.00215
S1 Char S1 KB4	-7.91295E-4	0.00131	-0.60266	0.56015	0.05	0	-0.00372	0.00213
S1 Char Narrowleaf	-0.00396	0.00131	-3.01277	0.01306	0.05	1	-0.00688	-0.00103
S1 Zam S1 KB3	-5.59673E-4	0.00131	-0.42625	0.67895	0.05	0	-0.00349	0.00237
S1 Zam S1 KB4	-5.8035E-4	0.00131	-0.442	0.66789	0.05	0	-0.00351	0.00235
S1 Zam Narrowleaf	-0.00374	0.00131	-2.85211	0.01719	0.05	1	-0.00667	-8.19282E-4
S1 Zam S1 Char	2.10945E-4	0.00131	0.16066	0.87556	0.05	0	-0.00271	0.00314

Sig equals 1 indicates that the difference of the means is significant at the 0.05 level.
Sig equals 0 indicates that the difference of the means is not significant at the 0.05 level.

Figure B-1. ANOVA and LSD analysis conducted with the help of Dr. Ying-Hsuan Lin.

APPENDIX C
LOCATION OF GC/EI-MS AND DTT ASSAY RAW DATA

Files are stored on multiple devices in the Surratt Lab for future work and analysis. The GC/EI-MS computer that operates the system has one copy of all data for that specific analysis. On the DESKTOP, the folder titled "MW" contains all experiments run during this timeframe. The second set of data is backed up on the IBM computer in the back left of the Surratt lab at UNC. The figures below show how to access the files:

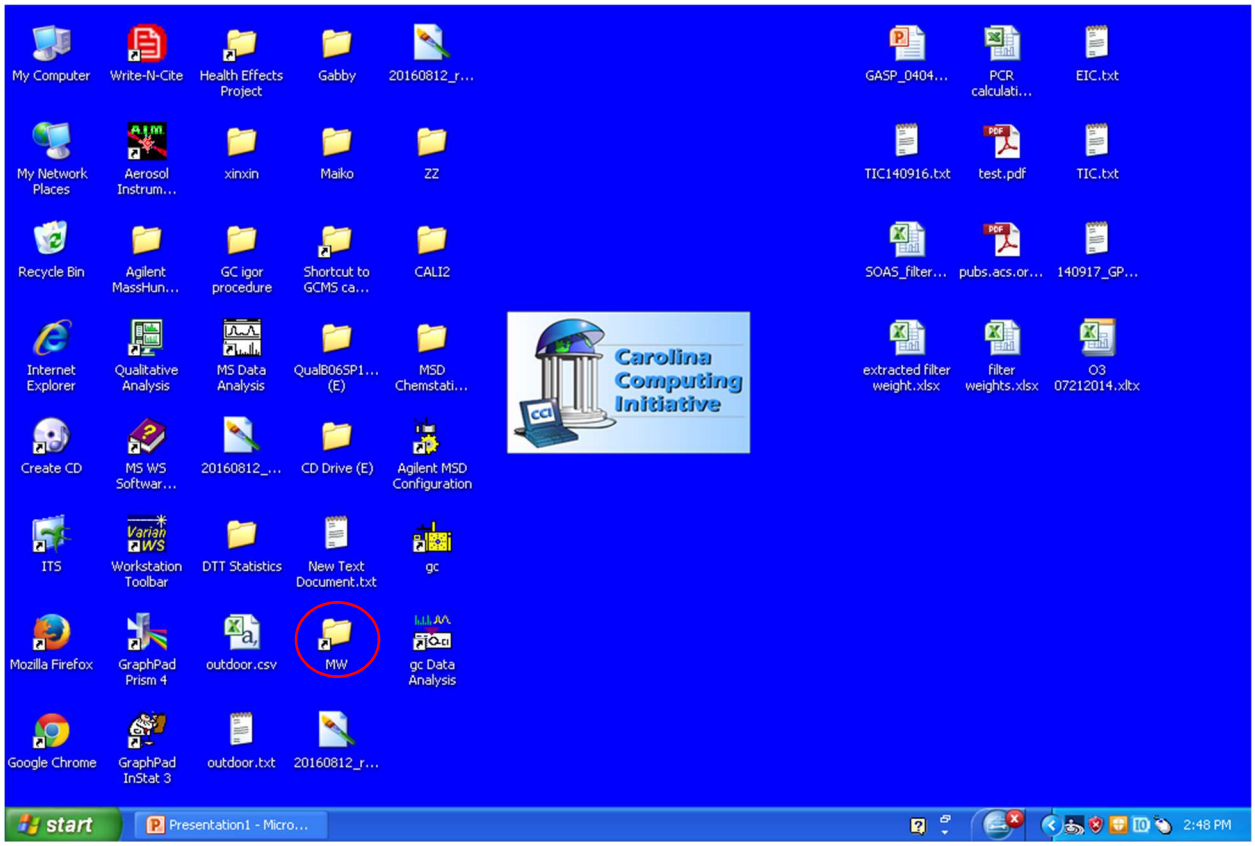

Figure C-1. Location of shortcut to access all GC/EI-MS data.

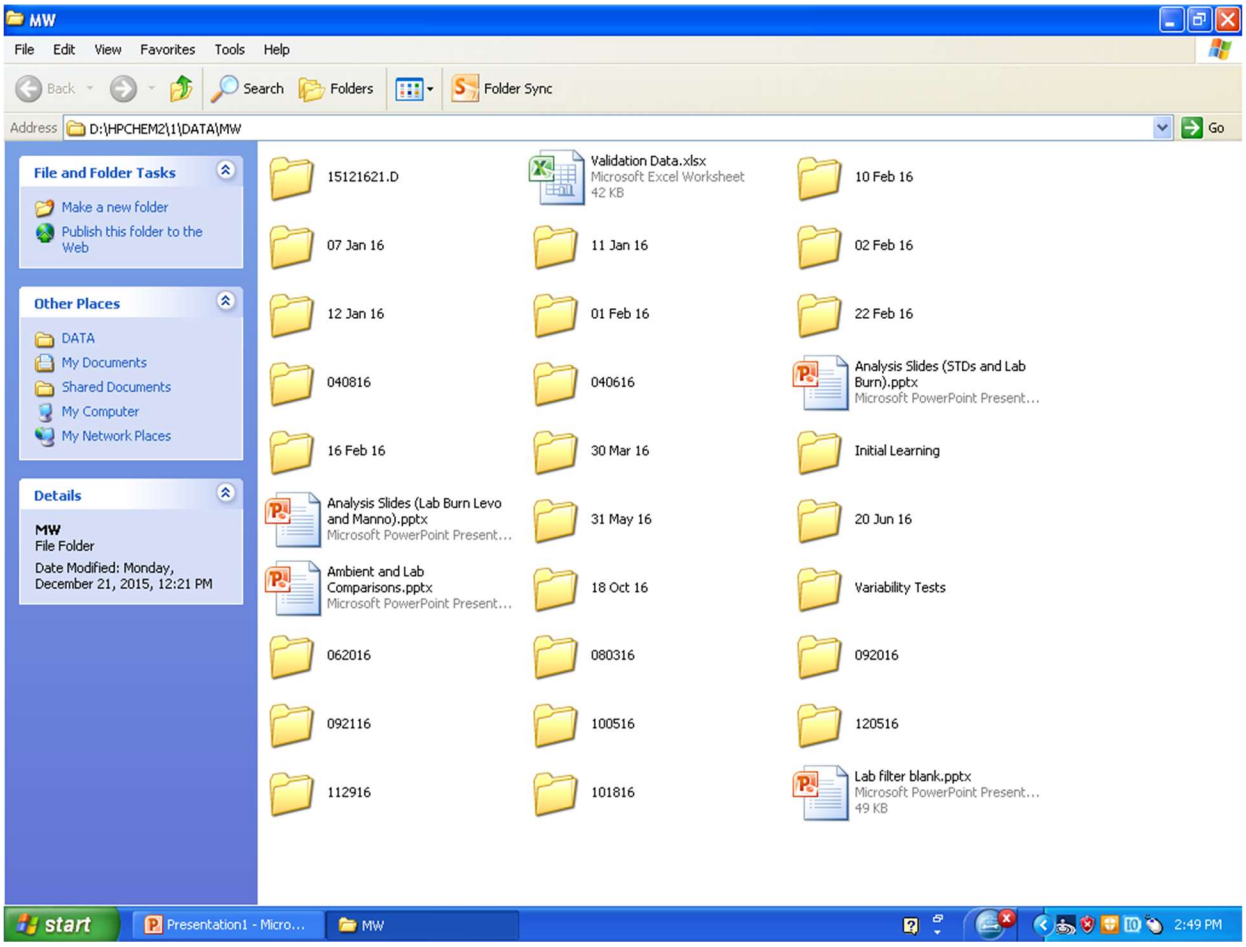

Figure C-2. Location of all GC/EI-MS data. Arranged in dates and PowerPoint slides.

All DTT Assay results are backed up on the IBM Thinkpad attached to the UV-Spectrophotometer in the Turpin Research Lab at UNC. All files are located in the shortcut labeled “MW” on the DESKTOP.

APPENDIX D
BROWN CARBON SUPPLEMENTAL DATA

ug/m3	365 nm RT 7.5 - 9.5 min								
EXP#	C10H9O4-	C9H5O3-	C8H7O3-	C6H11O4S-	C10H7O4-	C9H7O3-	C9H9O4-	C11H11O5-	C6H5O3-
1	756.43336	220.4155559	1474.327924	0	118.0622672	316.8939321	370.2997448	14.93068109	4.391759694
2	1524.2644	350.1704218	3981.418246	13.14555975	0	648.5031217	1155.139978	34.8447039	18.48557213
3	451.39642	210.6463585	1037.451196	0	132.653436	199.8103271	443.8317383	17.1904661	0
4	1617.6608	320.7458916	3399.510492	4.993814212	255.3228898	651.0404229	1599.343792	55.7254641	16.36583313
5	1870.9723	452.1435635	4906.969802	11.51118114	1577.763551	734.4331791	1768.420092	48.65662157	28.15621421
6	654.3306	171.6360074	3236.015883	3.785490983	142.0270265	815.1491503	545.3983607	4.724124423	48.27495438
7	272.29396	118.2812006	1771.341345	0	0	438.3613502	1069.756718	4.513641197	37.200495
8	541.43699	1124.186306	2718.532706	0	0	791.4360456	1108.213853	3.514072687	48.4214781
9	632.25119	117.7138657	1373.453169	0	0	252.4076389	435.1092746	21.86583058	15.14278643
10	661.42391	121.8631878	1461.287757	0	0	259.1776375	331.0899458	20.80060845	26.99350133
11	536.76037	145.9734901	1296.675562	0	0	203.5926179	330.5800987	17.97035482	10.48484521
12	1142.7101	167.7771144	2584.843595	0	0	291.4502881	746.3260097	48.21990774	17.58468577
13	1367.8347	188.467758	3581.985864	0	0	489.7917262	814.1195196	61.35043828	23.40797974

Figure D-1. BrC Constituents at 365 nm 7.5 to 9.5 min retention time.

365 nm RT 11.5 - 12.0 min										
C13H15O4-	C13H13O6S-	C12H13O7S-	C18H19O5S-	C23H21O7-	C15H7O5-	C6H4NO3-	C7H6NO3-	C6H4NO4-	C7H6NO4-	Sum_365nm_ug
0	0	0	0	38.80271557	0	0	0	0	0	3.31E+03
116.375883	18.8468665	7.815820464	4.568919678	0	32.19780714	0	0.02622837	0	0	7.91E+03
38.732738	11.30364506	3.584077524	0	0	114.3538011	0	0.003093176	0	0	2.66E+03
0	0	0	14.18663276	0	0	0	0	0.164845802	0	7.94E+03
0	15.64981874	0	0	0	0	0	0	0	0	1.14E+04
0	0	0	0	0	0	0	0	0.207584088	0.012793907	5.62E+03
0	0	0	0	0	0	0	0	0.137709523	0	3.71E+03
0	0	0	0	0	0	0	0	0.508766305	0	6.34E+03
0	0	0	0	0	0	0.037821212	0	0	0	2.85E+03
0	0	0.530034046	0	0	0	0.037084469	0	0	0	2.88E+03
0	0	0	2.57718602	0	0	0.032344302	0	0	0	2.54E+03
0	0	0	0	0	0	0.099295854	0	0	0	5.00E+03
0	0	0	0	0	0	0.043228992	0	0.145642686	0	6.53E+03

Figure D-2. BrC Constituents at 365 nm with 11.5 to 12.0 min retention time.

400 nm RT 5.0 - 7.5 min			
C5H7O4-	C7H7O3-	C14H17O2S-	Sum_400nm_ug/m
	0	0	0.00
	0	0	0.00
	0	0	0.00
	0	0	0.00
	381.0980753	0	381.10
	388.865715	1.778535718	390.64
	538.0153295	0	538.02
	808.5482143	0	808.55
	74.88355924	0	74.88
	73.8192248	0	73.82
	73.11534359	0	73.12
	166.043522	0	166.04
	229.2876904	0	229.29

Figure D-3. BrC Constituents at 400 nm with 5.0 to 7.5 min retention time.

500 nm RT 10.0 - 11.0 min									
C9H11O2-	C11H9O3-	C10H9O3-	C8H9O3S-	C12H17O4S-	C12H17O5S-	C17H17O5-	C10H11O3-	C12H9O2-	Sum_500nm_ug/m
0	0	0	0	0	0	0	46.49240409	128.7809863	175.27
0	0	0	2.894751012	0	5.866832869	0	83.85907235	212.8173887	305.44
0	0	0	0	0	3.1972347	0	0	63.32556185	66.52
558.4511583	0	419.3491381	3.420048192	0	0	0	90.59825504	228.3930726	1300.21
610.0868143	0	0	0	0	0	0	85.902637	0	695.99
720.8406717	172.4406624	411.1424992	6.881686441	9.89438669	8.9946716	7.420648212	122.9520959	65.9029733	1526.47
506.0440335	164.6410082	336.2047763	0	0	0	0	282.4716597	72.14532631	1361.51
1619.170968	428.701145	332.7442849	0	0	0	0	402.9671995	81.84467671	2865.43
0	0	0	0	0	0	0	45.8931967	78.97347955	124.87
0	0	0	0	0	0	0	59.73191836	70.55865438	130.29
0	120.0182182	139.6625491	0	0	0	0	36.42389163	54.33107543	350.44
0	0	0	0	0	0	0	41.1054588	84.51299351	125.62
0	0	0	0	0	6.419566136	0	102.8892315	0	109.31

Figure D-4. BrC Constituents at 500 nm with 10.0 to 11.0 min retention time.

580 nm RT 10.0 - 12.0 min										
C11H13O5S-	C15H19O6S-	C11H13O6S-	C14H17O4-	C14H13O4-	C10H17O4S-	C10H13O2-	C16H15O4-	C15H22N3O2-	Sum_580nm_ug/m	BB_sumBrC_ug_m3
18.69569088	0	0	0	0	0	0	0	0	18.70	3508.53
46.49120219	39.20573128	34.70273339	35.32927408	0	26.22837011	0	0	0	181.96	8393.20
0	15.67202277	10.28826962	7.077756868	0	3.093175678	0	0	0	36.13	2763.61
0	25.38474345	18.2033524	54.43759826	0	0	164.8458016	0	0	262.87	9498.14
0	17.95966215	0	29.26801915	0	0	0	0	0	47.23	12538.99
0	0	0	0	0	0	207.5840879	12.79390679	3.656773698	224.03	7762.71
0	0	0	0	0	0	137.7095234	0	11.35376147	149.06	5760.47
0	0	0	0	0	0	508.7663046	0	0	508.77	10518.99
0	0	0	0	37.82121166	0	0	0	0	37.82	3085.55
4.443422817	0	1.24357683	0	37.08446872	0	0	0	0	42.77	3130.08
0	0	0	0	32.34430218	0	0	0	0	32.34	3000.54
0	0	0	0	99.29585376	0	0	0	0	99.30	5389.97
0	0	0	24.0355681	43.22899196	0	145.6426864	0	0	212.91	7078.65

Figure D-5. BrC Constituents at 580 nm with 10.0 to 12.0 min retention time, sum of all constituents is the final column.

REFERENCES

Akagi, S.K.; Yokelson, R.J.; Wiedinmyer, C.; Alvarado, M.J.; Reid, J.S.; Karl, T.; Crounse J.D.; Wennberg, P.O.; (2011). Emission Factors for open and domestic biomass burning for use in atmospheric models. *Atmos. Chem. Phys., 11*, 4039-4072.

Andreae, M. O.; Merlet, P., (2001). Emission of trace gases and aerosols from biomass burning. *Global Biogeochem. Cycles, 15*(4), 955–966.

Bell, M.L., (2012). Assessment of the Health Impacts of Particulate Matter Characteristics. *Research Report 161*. Health Effects Institute, Boston, MA.

Bernstein, J.A.; Alexis, N.; Barnes, C.; Bernstein, I.L.; Nel, A.; Peden, D.; Diaz-Sanchez, D.; Tarlo, S.M.; Williams, P.B.; (2004). Health effects of air pollution. *American Academy of Allergy, Asthma, and Immunology*, 1116-1123.

Bond, T. C.; Streets, D.G.; Yarber, K.F.; Nelson, S.M.; Woo, J.H.; Klimont, Z., (2004). A technology-based global inventory of black and organic carbon emissions from combustion, *J. Geophys. Res., 109*, D14203.

Bond, T. C., et al. (2013). Bounding the role of black carbon in the climate system: A scientific assessment. *J. Geophys. Res. Atmos., 118*, 5380–5552.

Budisulistiorini, S.H.; Li, X.; Bairai, S.T.; Renfro, J.; Liu, Y.; Liu, Y.J.; McKinney, K.A.; Martin, S.T; McNeill, V.F.; Pye, H.O.T.; Nenes, A.; Neff, M.E.; Stone, E.A.; Mueller, S.; Knote, C.; Shaw, S.L.; Zhang, Z.; Gold, A.; Surratt, J.D., (2015). Examining the effects of anthropogenic emissions on isoprene-derived secondary organic aerosol formation during the 2013 Southern Oxidant and Aerosol Study (SOAS) at the Look Rock, Tennessee ground site. *Atmos. Chem. Phys., 15*, 8871-8888.

Budisulistiorini, S.H.; Riva, M.; Williams, M.; Chen, J.; Itoh, M.; Surratt, J.D.; Kuwata, M., (2017). Light-absorbing brown carbon aerosol constituents from combustion of Indonesian peat and biomass. *Environ. Sci. Technol., #*, pp.

Cho, A. K., Sioutas, C., Miguel, A. H., Kumagai, Y., Schmitz, D. A., Singh, M., et al. (2005). Redox activity of airborne particulate matter at different sites in the Los Angeles Basin. *Environmental Research, 99*(1), 40-47.

Crutzen, P.J.; Andreae, M.O., (1990). Biomass Burning in the Tropics: Impact on Atmospheric Chemistry and Biogeochemical Cycles. *Science, New Series, 250* (4988), 1669-1678.

Forster, P., V. Ramaswamy, P. Artaxo, T. Berntsen, R. Betts, D.W. Fahey, J. Haywood, J. Lean, D.C. Lowe, G. Myhre, J. Nganga, R. Prinn, G. Raga, M. Schulz and R. Van Dorland, 2007: Changes in Atmospheric Constituents and in Radiative Forcing. In: Climate Change 2007: The Physical Science Basis. Contribution of Working Group I to the Fourth Assessment Report of the Intergovernmental Panel on Climate Change [Solomon, S., D. Qin, M. Manning, Z. Chen, M. Marquis, K.B. Averyt, M.Tignor and H.L. Miller (eds.)]. Cambridge University Press, Cambridge, United Kingdom and New York, NY, USA.

Fröhlich, R.; Cubison, M. J.; Slowik, J. G.; Bukowiecki, N.; Prévôt, A. S. H.; Baltensperger, U.; Schneider, J.; Kimmel, J. R.; Gonin, M.; Rohner, U.; Worsnop, D. R.; Jayne, J. T. (2013). The ToF-ACSM: a portable aerosol chemical speciation monitor with TOFMS detection. *Atmos. Meas. Tech., 6*, 3225-3241.

Guenther, A.; Karl, T.; Harley, P.; Wiedinmyer, C.; Palmer, P. I.; Geron, C., (2006). Estimates of global terrestrial isoprene emissions using MEGAN (Model of Emissions of Gases and Aerosols from Nature). *Atmos. Chem. Phys., 6*, 3181-3210.

Hallquist, M.; Wenger, J. C.; Baltensperger, U.; Rudich, Y.; Simpson, D.; Claeys, M.; Dommen, J., Donahue, N. M.; George, C.; Goldstein, A. H.; Hamilton, J. F.; Herrmann, H.; Hoffmann, T.; Iinuma, Y.; Jang, M.; Jenkin, M. E.; Jimenez, J. L.; Kiendler-Scharr, A.; Maenhaut, W.; McFiggans, G.; Mentel, Th. F.; Monod, A.; Prévôt, A. S. H.; Seinfeld, J. H.; Surratt, J. D.; Szmigielski, R.; Wildt, J., (2009). The formation, properties and impact of secondary organic aerosol: current and emerging issues. *Atmos. Chem. Phys., 9*, 5155-5236.

Hatch, L.E.; Luo, W.; Pankow, J.F.; Yokelson, R.J.; Stockwell, C.E.; Barsanti, K.C. (2015). Identification and quantification of gaseous organic compounds emitted from biomass burning using two-dimensional gas chromatography-time-of-flight mass spectrometry. *Atmos. Chem. Phys., 15*, 1865-1899.

Hennigan, C.J.; Sullivan, A.P.; Collett Jr., J.L.; Robinson, A.L., (2010). Levoglucosan stability in biomass burning particles exposed to hydroxyl radicals. *Geophys. Res. Letters, 37*, 1-4.

Hobbs, P.V.; Reid, J.S.; Kotchenruther, R.A.; Ferek, R.J.; Weiss, R., (1997). Direct Radiative Forcing by Smoke from Biomass Burning. *Science, 275* (5307), 1777-1778.

Hu, Q-H.; Xie, Z-Q.; Wang, X-M.; Kang, H.; Zhang, P., (2013). Levoglucosan indicates high levels of biomass burning aerosols over oceans from the Arctic to Antarctic. *Sci. Rep., 3* (3119), 1-7.

Jacobson, M. Z. (2014), Effects of biomass burning on climate, accounting for heat and moisture fluxes, black and brown carbon, and cloud absorption effects, *J. Geophys. Res. Atmos., 119*, 8980–9002.

Karl, T.R.; Melillo, J.M.; Peterson, T.C., (2009). Global Climate Change Impacts in the United States. Cambridge University Press.

Kleindienst T.E.; Conver, T.S.; McIver, C.D.; Edney, E.O. (2004). Determination of Secondary Organic Aerosol Products from the Photooxidation of Toluene and their Implications in Ambient PM2.5. *Journal of Atmospheric Chemistry 47*, 79-100.

Kramer, A. J.; Rattanavaraha, W.; Zhang, Z.; Gold, A.; Surratt, J. D.; Lin, Y.-H. (2016) Assessing the oxidative potential of isoprene-derived epoxides and secondary organic aerosol. *Atmospheric Environment 130*, 211-218.

Laskin, A.; Laskin, J.; Nizkorodov, S., (2015). Chemistry of Atmospheric Brown Carbon. *Chemical Reviews, 115* (10), 4335-4382.

Lauraguais, A.; Coeur-Tourneur, C.; Cassez, A.; Deboudt, K.; Formentin, M.; Choel, M.; (2014). Atmospheric reactivity of hydroxyl radicals with guaiacol (2-methoxyphenol), a biomass burning emitted compound: Secondary organic aerosol formation and gas-phase oxidation products. Atmos. Environ., 86, 155-163.

Li, N., Sioutas, C., Cho, A., Schmitz, D., Misra, C., Sempf, J., Wang, M., Oberley, T., Froines, J., Nel , A. (2003a). Ultrafine particulate pollutants induce oxidative stress and mitochondrial damage. *Environ. Health Perspect. 111* (4), 455-460.

Li, N., Hao, M., Phalen, R.F., Hinds, W.C., Nel, A.E. (2003b). Particulate air pollutants and asthma, a paradigm for the role of oxidative stress in PM-induced adverse health effects. *Clin. Immunol. 109*, 250-265.

Li, N., Xia, T., Nel, A. E., (2008). The role of oxidative stress in ambient particulate matter-induced lung diseases and its implications in the toxicity of engineered nanoparticles. *Free Radical Biology and Medicine, 44* (9), 1689-1699.

Li, Q., Wyatt, A., Kamens, R.M., (2009). Oxidant generation and toxicity enhancement of aged-diesel exhaust. *Atmos. Environ., 43* (5), 1037-1042.

Lighty, J.S.; Veranth, J.M.; Sarofim, A.F., (2000). Combustion Aerosols: Factors Governing Their Size and Composition and Implications to Human Health, *Journal of the Air & Waste Management Association, 50* (9), 1565-1618.

Lin, G.; Penner, J. E.; Sillman, S.; Taraborrelli, D.; and Lelieveld, J., (2012). Global modeling of SOA formation from dicarbonyls, epoxides, organic nitrates and peroxides. *Atmos. Chem. Phys., 12*, 4743-4774.

Mao, J.; Horowitz, L.W.; Vaishali, N.; Fan, S.; Liu, J.; Fiore, A., (2013). Sensitivity of tropospheric oxidants to biomass burning emissions: implications for radiative forcing. *Geophysical Research Letters, 40*, 1241-1246.

McWhinney, R.D., Badali, K., Liggio, J., Li, S.-M., Abbatt, J.P.D., (2013). Filterable redox cycling activity: a comparison between diesel exhaust particles and secondary organic aerosol constituents. *Environ. Sci. Technol., 47*, 3362-3369.

Mochida, M.; Kawamura, K.; Fu, P.; Takemura, T.; (2010). Seasonal variation of levoglucosan in aerosols over the western North Pacific and its assessment as a biomass-burning tracer. *Atmos. Environ., 44* (29), 3511-3518.

Pope, C.A.; Dockery, D.W., (2006). Health Effects of Fine Particulate Air Pollution: Lines that Connect. *J. Air & Waste Manage. Assoc., 56*, 709-742.

Poster, D.L.; Schantz, M.M.; Sander, L.C.; Wise, S.A., (2006). Analysis of polycyclic aromatic hydrocarbons (PAHs) in environmental samples: a critical review of gas chromatographic (GC) methods. *Anal. Bioanal. Chem., 386* (4), 859-881.

Rattanavaraha, W.; Rosen, E.; Zhang, H.; Li, Q.; Pantong, K.; Kamens, R.M., (2011). The reactive oxidant potential of different types of aged atmospheric particles: an outdoor chamber study. *Atmos. Environ., 45*, 3848-3855.

Schauer, J.J.; Kleeman, M.J.; Cass, G.R.; Simoneit, B.R.T., (2001). Measurement of Emissions from Air Pollution Sources. 3. C_1−C_{29} Organic Compounds from Fireplace Combustion of Wood. *Environ. Sci. Technol., 35* (9), 1716-1728.

Simoneit, B.R.T.; Schauer, J.J.; Nolte, C.G.; Oros, D.R.; Elias, V.O.; Fraser, M.P.; Rogge, W.F.; Cass, G.R., (1999). Levoglucosan, a tracer for cellulose in biomass burning and atmospheric particles. *Atmos. Environ., 33* (2), 173-182.

Stockwell, C.E.; Veres, P.R., Williams, J.; Yokelson, R.J., (2015). Characterization of biomass burning emissions from cooking, peat, crop residue, and other fuels with high-resolution proton-transfer-reaction time-of-flight mass spectrometry. *Atmos. Chem. Phys., 15*, 845-865.

Surratt, J.D.; Chan, A.W.H.; Eddingsaas, N.C.; Chan, M.; Loza, C.L.; Kwan, A.J.; Hersey, S.P.; Flagan, R.C.; Wennberg, P.O.; Seinfeld, J.H., (2010). Reactive intermediates revealed in secondary organic aerosol formation from isoprene. PNAS, 107 (15), 6640-6645.

Tao, F.; Gonzalez-Flecha, B.; Kobzik, L., (2003). Reactive oxygen species in pulmonary inflammation by ambient particles. *Free Radical Biology & Medicine, 35* (4), 327-340.

Usup, A.; Hashimoto, Y.; Takahashi, H.; Hayasaka, H., (2004). Combustion and Thermal Characteristics of peat fire in tropical peatland in Central Kalimantan, Indonesia. *Tropics, 14* (1), 1-19.

Verma, V.; Polidori, A.; Schauer, J.J.; Shafer, M.M.; Cassee, F.R.; Sioutas, C., (2009). Physicochemical and Toxicological Profiles of Particulate Matter in Los Angeles during the October 2007 Southern California Wildfires. Environ. Sci. Technol., 43, 954-960.

Verma, V., Rico-Martinez, R., Kotra, N., King, L., Liu, J., Snell, T.W., Weber, R.J., (2012). Contribution of water-soluble and insoluble components and their hydrophobic/ hydrophilic subfractions to the reactive oxygen species-generating potential of fine ambient aerosols. *Environ. Sci. Technol., 46*, 11384-11392.

Verma, V.; Fang, T.; Xu, L.; Peltier, R.E.; Russell, A.G.; Ng, N.L.; Weber, R.J., (2015). Organic aerosols associated with the generation of reactive oxygen species (ROS) by water-soluble PM2.5. *Environ. Sci. Technol., 49*, 4646-4656.

Vreeland, H.; Schauer, J.J.; Russell, A.G.; Marshall, J.D.; Fushimi, A.; Jain, G.; Sethuraman, K.; Verma, V.; Tripathi, S.N.; Bergin, M.H., (2016). Chemical characterization and toxicity of particulate matter emissions from roadside trash combustion in urban India. *Atmos. Environ., 147*, 22-30.

World Health Organization (WHO). WHO Air quality guidelines for particulate matter, ozone, nitrogen dioxide and sulfur dioxide. Global update 2005, Summary of Risk Assessment.

Wilhelm, M.; Ghosh, J.; Su, J.; Cockburn, M.; Jerrett, M.; Ritz, B., (2012). Traffic-related air toxics and term low birth weight in Los Angeles County, California. *Environ Health Perspect., 120*, 132–138.

Xing, Y.; Xu, Y.; Shi, M.; Lian, Y., (2016). The impact of PM2.5 on the human respiratory system. *Journal of Thoracic Disease, 8* (1), E69-E74.

Yang, A., Jedynska, A., Hellack, B., Kooter, I., Hoek, G., Brunekreef, B., Kuhlbusch, T.A.J., Cassee, F.R., Janssen, N.A.H., (2014). Measurement of the oxidative potential of PM2.5 and its constituents: the effect of extraction solvent and filter type. *Atmos. Environ., 83*, 35-42.

Zhang, H.; Surratt, J. D.; Lin, Y. H.; Bapat, J.; Kamens, R. M., (2011). Effect of relative humidity on SOA formation from isoprene/NO photooxidation: enhancement of 2-methylglyceric acid and its corresponding oligoesters under dry conditions. *Atmos. Chem. Phys., 11*, 6411-6424.

Zhang, T.; Claeys, M.; Cachier, H.; Dong, S.; Wang, W.; Maenhaut, W.; Liu, X., (2008). Identification and estimation of the biomass burning contribution to Beijing aerosol using levoglucosan as a molecular marker. *Atmos. Environ., 42*, 7013-7021.